Mixed Convolved Action Variational Methods for Poroelasticity

Bradley T. Darrall
Mechanical and Aerospace Engineering
University at Buffalo, State University of New York
Buffalo, NY, USA 14260

Gary F. Dargush
Mechanical and Aerospace Engineering
University at Buffalo, State University of New York
Buffalo, NY, USA 14260
Email: gdargush@buffalo.edu

Abstract

Although Lagrangian and Hamiltonian analytical mechanics represent perhaps the most remarkable expressions of the dynamics of a mechanical system, these approaches also come with limitations. In particular, there is inherent difficulty to represent dissipative processes and the restrictions placed on end point variations are not consistent with the definition of initial value problems. The present work on the time domain response of poroelastic media extends the recent formulations of the mixed convolved action. The action in this proposed approach is formed by replacing the inner product in Hamilton's principle with a time convolution. As a result, dissipative processes can be represented in a natural way and the required constraints on the variations are consistent with the actual initial and boundary conditions of the problem. The variational formulation developed here employs temporal impulses of velocity, effective stress, pore pressure and pore fluid mass flux as primary variables in this mixed approach, which also uses convolution operators and fractional calculus to achieve the desired characteristics. The resulting mixed convolved action is formulated directly in the time domain to develop a new stationary principle for poroelasticity, which applies to dynamic poroelastic and quasistatic consolidation problems alike. By discretizing the mixed convolved action using the finite element method over both space and time, new computational mechanics formulations are developed. Here, this formulation is implemented for the two-dimensional case and several numerical examples of dynamic poroelasticity are presented to validate the approach.

1 Introduction

While Hamilton's principle of stationary action has long been regarded as perhaps the most elegant formulation describing the dynamics of a physical system [1-4], it also has notable shortcomings, mainly the inability to model dissipative phenomena and the inconsistency of variations with respect to the specified initial conditions. The former difficulty was noticed early on and in order to accommodate irreversible phenomena, a Rayleigh dissipation function can be introduced, along with a prescribed set of ad hoc rules for taking the variations [5-8]. While these methods have enjoyed great success for a range of problems, it is well known that such formulations do not lead to true variational principles in a strict mathematical sense.

In order to resolve these main shortcomings of Hamilton's principle, Gurtin [9-11] and Tonti [12-15] replaced the inner product operators over time with temporal convolutions. The usual inner products appearing in Hamilton's principle require zero variations at both endpoints and, thus, actually are consistent with boundary value problems. On the other hand, the required restrictions on the variations for convolution-based functionals align well with the given data for initial value problems. Furthermore, the convolution operators allow for the inclusion of dissipative processes without any ad hoc rules for the definition of stationarity of the functional. Along these lines, Oden and Reddy [16] derived a number of continuum convolution-based formulations, including elastodynamics and thermoelasticity, with the latter incorporating the effects of dissipation. In all of this convolution-based work, the objective was to recover the governing partial differential equations as the Euler-Lagrange equations of the variational formulation.

In the present work, we strive to recover the complete definition of the initial/boundary value problem for poroelasticity, including not only the governing partial differential equations, but also the boundary and initial conditions, as the Euler-Lagrange equations of a single scalar action functional. We denote this functional as the mixed convolved action (MCA), which has been developed in recent work for linear

lumped parameter single degree of freedom dynamical systems [17, 18], linear elastodynamic continua [19] and heat diffusion [20]. Here we extend the stationary principle of mixed convolved action to consider the response of linear poroelastic media, based upon the Biot theory [21-24]. Notably, this novel formulation is demonstrated to recover all of the governing partial differential equations, boundary conditions and initial conditions of Biot poroelasticity as the Euler-Lagrange equations associated with the mixed convolved action functional. This MCA functional is written in terms of mixed impulsive variables, fractional derivatives and convolutions. Thus, a single scalar functional captures all of the conservative and non-conservative aspects of poroelastic response and a new stationary principle is derived without the need for ad hoc assumptions concerning the variations.

Beyond the theoretical significance of the principle of stationary mixed convolved action for linear poroelastic response, these concepts lead directly to the development of novel computational methods involving finite element representations over both space and time. The present paper includes the theoretical formulation in terms of primary mixed variables, which include the impulses of velocity, pressure, stress and flux. From analysis of the mixed convolved action, the former two variables require C^0 continuity over space, while the latter two may be defined with C^{-1} spatial continuity. Thus, for a two-dimensional numerical implementation, displacement and pressure impulse can be represented using standard three-node linear triangular finite elements, with stress impulse and relative pore fluid displacement defined by independent constants over each finite element. Meanwhile, all four primary impulsive variables require C^0 temporal continuity. Consequently, linear temporal shape functions can be used to represent all of the primary variables over each time step.

Before providing our detailed mixed convolved action formulation, we should mention several other approaches that have been offered to accommodate non-conservative processes within a variational

framework. This includes approaches based upon mirrored systems [25], fractional calculus [26, 27], bracket formalisms [28-31] and the related GENERIC framework [32-35].

We begin our development in the next section with a review of the governing equations of Biot poroelasticity. Then, in Section 3, the focus shifts to the theoretical development of the new stationary variational principle for poroelasticity in the time domain. Next, to solve general problems of transient poroelasticity, the action principle is discretized in Section 4, using the finite element method in both space and time. Finally, Section 5 provides some conclusions.

2 Fundamental Relations

As a starting point for the development of a pure variational statement for the problem of dynamic continuum poroelasticity, in this section, we present the basic governing equations. In particular, here we consider viscous flow of a pore fluid as a dissipative process and develop a mixed convolved action formalism for infinitesimal poroelasticity. In a way, this formalism can be regarded as the evolution of previous work on the poroelastic problem in Reference [36], which used instead an inner product action variation based upon Lagrangian energy and Rayleigh dissipation functionals.

For a continuum governed by infinitesimal poroelasticity theory, let v_i and σ_{ij}^e represent the velocity and effective stress of the solid skeleton, respectively. Meanwhile, for the pore fluid, let p and q_i denote the pore pressure and the average velocity relative to the solid skeleton, respectively. Then, the impulses of these four quantities are defined as u_i, J_{ij}, π and w_i, respectively, where

$$u_i(t) = \int_0^t v_i(t)dt \tag{1a}$$

$$J_{ij}(t) = \int_0^t \sigma_{ij}^e(t)dt = \int_0^t C_{ijkl}\varepsilon_{kl}(t)dt \tag{1b}$$

$$\pi(t) = \int_0^t p(t)dt \tag{1c}$$

$$w_i(t) = \int_0^t q_i(t)dt \tag{1d}$$

Here, u_i is the solid skeleton displacement and w_i represents the average pore fluid displacement relative to the solid skeleton. A number of dynamic poroelastic formulations are written in terms of u_i and w_i as primary variables, including Biot [24], Predeleanu [37] and Manolis and Beskos [38]. However, following the approach taken in Reference [36], we instead consider mixed formulations written in terms of all four variables. Naturally, in the corresponding rate form, we have for these variables

$$\dot{u}_i = v_i \tag{2a}$$

$$\dot{J}_{ij} = \sigma_{ij}^e = C_{ijkl}\varepsilon_{kl} \tag{2b}$$

$$\dot{\pi} = p \tag{2c}$$

$$\dot{w}_i = q_i \tag{2d}$$

where σ_{ij}^e denotes the effective stress, ε_{ij} represents the total strain tensor and C_{ijkl} is the linear elastic constitutive tensor for the solid skeleton written in terms of drained properties. Meanwhile, the total stress σ_{ij} can be written in terms of the effective stress and pore pressure as

$$\sigma_{ij} = \sigma_{ij}^e - \beta_{ij} p \tag{3}$$

with β_{ij} representing a constitutive tensor for anisotropic poroelastic media relating to compressibility of the two-phase mixture, which reduces to $\beta_{ij} = \beta\delta_{ij}$ for the isotropic case.

In terms of these mixed variables, the governing differential equations for Biot dynamic poroelastic response over the domain Ω take the following form:

$$\rho_o \ddot{u}_k + \rho_f \ddot{w}_k - B_{ijk}\left(\dot{J}_{ij} - \beta_{ij}\dot{\pi}\right) = \overline{f}_k \tag{4a}$$

$$A_{ijkl}\ddot{J}_{kl} - B_{ijk}\dot{u}_k = 0 \tag{4b}$$

$$\frac{1}{Q}\dot{\pi} + B_i\dot{w}_i + \beta_{ij}B_{ijk}\dot{u}_k = \bar{\Gamma} \tag{4c}$$

$$\frac{\rho_f}{n}\ddot{w}_j + \rho_f\ddot{u}_j + \lambda_{ij}\dot{w}_i + B_j\dot{\pi} = 0 \tag{4d}$$

where ρ_s and ρ_f represent the mass density of the solid and fluid, respectively, while ρ_o is the mass density of the solid-fluid mixture, such that

$$\rho_o = (1-n)\rho_s + n\rho_f \tag{5}$$

Furthermore, n is the porosity and Q is the Biot parameter to account for compressibility of the two phase mixture. In addition, $\bar{f}_k$ represents a specified body force density, while $\bar{\Gamma}$ is a specified volumetric body source rate. The constitutive tensors A_{ijkl} and λ_{ij} are the inverses of the elastic moduli of the solid skeleton C_{ijkl} and the permeability κ_{ij}, respectively. The permeability, in turn, can be written as $\kappa_{ij} = k_{ij}/\eta$, where k_{ij} and η represent the specific permeability and pore fluid viscosity, respectively. Finally, B_i and B_{ijk} represent differential operators that are defined as

$$B_i = \frac{\partial}{\partial x_i} \tag{6a}$$

$$B_{ijk} = \frac{1}{2}\left(\delta_{ik}\delta_{jq} + \delta_{iq}\delta_{jk}\right)\frac{\partial}{\partial x_q} \tag{6b}$$

Notice that equation (4a) represents linear momentum balance, (4b) is the linear elastic effective stress-strain constitutive relation in rate form and (4c) is the pore fluid balance equation with

$$\dot{\zeta} = -\dot{w}_{i,i} + \bar{\Gamma} \tag{7}$$

as the fluid content rate. The remaining governing equation (4d) represents an extended Darcy's law for pore fluid flow. For a detailed derivation of this particular governing equation, as well as an explicit description of its connection to Darcy's law the reader is referred to Refs. [23,24,51].

In addition to the governing differential equations, boundary conditions must be specified. For the simplest form, these can be written:

$$u_k = \bar{u}_k \quad \text{on} \quad \Gamma_v \tag{8a}$$

$$\dot{J}_{kj} n_j - \beta_{kj} \dot{\pi} n_j = \sigma_{kj} n_j = \bar{t}_k \quad \text{on} \quad \Gamma_t \tag{8b}$$

$$\pi = \bar{\pi} \quad \text{on} \quad \Gamma_p \tag{8c}$$

$$\dot{w}_i n_i = \bar{q} \quad \text{on} \quad \Gamma_q \tag{8d}$$

where $\bar{u}_k$ and $\bar{\pi}$ represent essential boundary conditions of displacement and pore pressure impulse applied on the surfaces Γ_v and Γ_p, respectively. Meanwhile, for the natural boundary conditions, $\bar{t}_k$ are the tractions specified on the portion of the surface Γ_t, while $\bar{q}$ represents the specified normal relative fluid volume discharge on Γ_q.

Then, to complete the definition of the Biot poroelastic problem, initial conditions are required. In mixed variables, these take the following form at time zero:

$$\rho_o \dot{u}_k(0) + \rho_f \dot{w}_k(0) - B_{ijk}\left(J_{ij}(0) - \beta_{ij}\pi(0)\right) = \bar{j}_k(0) \tag{9a}$$

$$A_{ijkl} \dot{J}_{kl}(0) - B_{ijk} u_k(0) = 0 \tag{9b}$$

$$\frac{1}{Q}\dot{\pi}(0) + B_i w_i(0) + \beta_{ij} B_{ijk} u_k(0) = \bar{\Upsilon}(0) \tag{9c}$$

$$\frac{\rho_f}{n}\dot{w}_j(0) + \rho_f \dot{u}_j(0) + \lambda_{ij} w_i(0) + B_j \pi(0) = 0 \tag{9d}$$

where $\bar{j}_k$ and $\bar{\Upsilon}$ are the impulses of $\bar{f}_k$ and $\bar{\Gamma}$, respectively.

Interestingly, the corresponding quasistatic problem of linear Biot consolidation can be studied using the formulation above by ignoring the inertial contributions with the approximation that $\rho_o = \rho_f = 0$.

3 Mixed Convolved Action

As noted in the Introduction, previous mixed convolved action formulations have been developed for lumped parameter systems [17, 18] and continua [19, 20]. Here, we extend the MCA approach for poroelastic response, under both dynamic and quasistatic theory. Elements of this formulation can be found already in the mixed Lagrangian formalism (MLF) [36], where an underlying action is defined implicitly for Biot dynamic poroelasticity by identifying Lagrangian and dissipation functions. However, in [36], these functions are then integrated over time to provide an inner product-based variational formulation. Within this MLF, which was developed originally by Sivaselvan, Reinhorn and colleagues [39-41], the action in the presence of dissipative effects is never written in explicit form. Instead, special restricted variations are introduced following the Rayleigh dissipation approach to write the stationarity of the action, which then may be used to produce effective numerical algorithms for dynamical problems.

The mixed convolved action for this case can be written by starting from the definitions of the Lagrangian and Rayleigh dissipation functionals in equations (35)-(39) of Reference [36] and converting the inner products term by term to temporal convolutions. The result is a single real scalar functional I_{C_p} that can be written in the following form:

$$
\begin{aligned}
I_{C_P} &= \int_\Omega \left[\tfrac{1}{2} \dot{u}_k * (1-n) \rho_s \dot{u}_k \right] d\Omega \\
&+ \int_\Omega \left[\tfrac{1}{2} \left(\dot{u}_k + \frac{\dot{w}_k}{n} \right) * n \rho_f \left(\dot{u}_k + \frac{\dot{w}_k}{n} \right) \right] d\Omega \\
&- \int_\Omega \left[\tfrac{1}{2} \dot{J}_{ij} * A_{ijkl} \dot{J}_{kl} \right] d\Omega \\
&- \int_\Omega \left[\tfrac{1}{2} \dot{\pi} * \frac{1}{Q} \dot{\pi} - \tfrac{1}{2} \breve{w}_i * \lambda_{ij} \breve{w}_j \right] d\Omega \\
&+ \int_\Omega \left[\tfrac{1}{2} \left(\breve{J}_{ij} * B_{ijk} \breve{u}_k - \breve{u}_k * B_{ijk} \breve{J}_{ij} \right) \right] d\Omega \\
&- \int_\Omega \left[\tfrac{1}{2} \left(\beta_{ij} \breve{\pi} * B_{ijk} \breve{u}_k - \breve{u}_k * B_{ijk} \beta_{ij} \breve{\pi} \right) \right] d\Omega \\
&+ \int_\Omega \left[\tfrac{1}{2} \left(\breve{w}_i * B_i \breve{\pi} - \breve{\pi} * B_i \breve{w}_i \right) \right] d\Omega \\
&- \int_\Omega \left[\breve{u}_k * \breve{\breve{J}}_k \right] d\Omega + \int_\Omega \left[\breve{\pi} * \breve{\breve{\Upsilon}} \right] d\Omega \\
&- \int_{\Gamma_t} \tfrac{1}{2} \left[\breve{u}_k * \breve{\breve{\tau}}_k \right] d\Gamma + \int_{\Gamma_v} \tfrac{1}{2} \left[\breve{\tau}_k * \breve{\breve{u}}_k \right] d\Gamma \\
&- \int_{\Gamma_q} \tfrac{1}{2} \left[\breve{\pi} * \breve{\breve{w}} \right] d\Gamma + \int_{\Gamma_p} \tfrac{1}{2} \left[\breve{w} * \breve{\breve{\pi}} \right] d\Gamma
\end{aligned} \tag{10}
$$

with $w = w_i n_i$ and $\tau_i = J_{ji} n_j$. The superposed breve symbol represents a left Riemann-Liouville semi-derivative [42, 43], defined as

$$
\breve{f} = \left(\mathscr{D}_{0^+}^{1/2} f \right)(t) \equiv \frac{1}{\sqrt{\pi}} \frac{d}{dt} \int_0^t \frac{f(\tau)}{(t-\tau)^{1/2}} d\tau \tag{11}
$$

for any suitably continuous function $f(t)$, where the non-italic π is the ratio of the circumference to the diameter of a circle.

Notice from (11) that the semi-derivative operator also involves a convolution of the function $f(t)$ with a kernel $1/\sqrt{\pi t}$, so that many of the terms in the mixed convolved action in (10) are actually convolutions of convolutions. In particular, the first of those terms, with action density $\tfrac{1}{2} \breve{w}_i * \lambda_{ij} \breve{w}_j$, models the viscous dissipation. Here, we have the convolution of the semi-derivative of the relative displacement of the pore fluid $\breve{w}_i$ with itself through the inverse permeability tensor λ_{ij}. This captures the history dependence of

these irreversible processes, which is something that cannot be done within the classical Lagrangian inner product framework. Interestingly, all of the other terms involving semi-derivatives can be written with balanced orders of the time derivatives across the two distinct variables. As we shall see, this not only leads to a weak form with ideal properties, but also permits recovery of the complete initial/boundary value problem of dynamic poroelasticity.

The next step is to enforce stationarity of the mixed convolved action (10) by setting the first variation equal to zero. Despite the presence of both first- and semi-derivatives with respect to time, this operation is easily performed and the result can be written as follows:

$$
\begin{aligned}
\delta I_{C_P} = & \int_\Omega \left[\delta \dot{u}_k * (1-n) \rho_s \dot{u}_k \right] d\Omega \\
& + \int_\Omega \left[\left(\delta \dot{u}_k + \frac{\delta \dot{w}_k}{n} \right) * n \rho_f \left(\dot{u}_k + \frac{\dot{w}_k}{n} \right) \right] d\Omega \\
& - \int_\Omega \left[\delta \dot{J}_{ij} * A_{ijkl} \dot{J}_{kl} \right] d\Omega \\
& - \int_\Omega \left[\delta \dot{\pi} * \frac{1}{Q} \dot{\pi} - \delta \breve{w}_i * \lambda_{ij} \breve{w}_j \right] d\Omega \\
& + \int_\Omega \left[\tfrac{1}{2} \left(\delta \breve{J}_{ij} * B_{ijk} \breve{u}_k - \breve{u}_k * B_{ijk} \delta \breve{J}_{ij} \right) \right] d\Omega \\
& + \int_\Omega \left[\tfrac{1}{2} \left(\breve{J}_{ij} * B_{ijk} \delta \breve{u}_k - \delta \breve{u}_k * B_{ijk} \breve{J}_{ij} \right) \right] d\Omega \\
& - \int_\Omega \left[\tfrac{1}{2} \left(\beta_{ij} \delta \breve{\pi} * B_{ijk} \breve{u}_k - \breve{u}_k * B_{ijk} \beta_{ij} \delta \breve{\pi} \right) \right] d\Omega \\
& - \int_\Omega \left[\tfrac{1}{2} \left(\beta_{ij} \breve{\pi} * B_{ijk} \delta \breve{u}_k - \delta \breve{u}_k * B_{ijk} \beta_{ij} \breve{\pi} \right) \right] d\Omega \\
& + \int_\Omega \left[\tfrac{1}{2} \left(\delta \breve{w}_i * B_i \breve{\pi} - \breve{\pi} * B_i \delta \breve{w}_i \right) \right] d\Omega \\
& + \int_\Omega \left[\tfrac{1}{2} \left(\breve{w}_i * B_i \delta \breve{\pi} - \delta \breve{\pi} * B_i \breve{w}_i \right) \right] d\Omega \\
& - \int_\Omega \left[\delta \breve{u}_k * \breve{\breve{j}}_k \right] d\Omega + \int_\Omega \left[\delta \breve{\pi} * \breve{\breve{\Upsilon}} \right] d\Omega \\
& - \int_{\Gamma_t} \tfrac{1}{2} \left[\delta \breve{u}_k * \breve{\breve{\tau}}_k \right] d\Gamma + \int_{\Gamma_v} \tfrac{1}{2} \left[\delta \breve{\tau}_k * \breve{\breve{u}}_k \right] d\Gamma \\
& - \int_{\Gamma_q} \tfrac{1}{2} \left[\delta \breve{\pi} * \breve{\breve{w}} \right] d\Gamma + \int_{\Gamma_p} \tfrac{1}{2} \left[\delta \breve{w} * \breve{\breve{\pi}} \right] d\Gamma = 0
\end{aligned}
\tag{12}
$$

By using classical and fractional integration-by-parts, we will show that (12) does indeed reproduce all of the elements of the initial/boundary value problem, but first let us establish the weak form to be used as the foundation for a corresponding time-space finite element method for dynamic poroelastic response. Examining the temporal derivatives in (12), we notice that terms appear in which first derivatives of all four field variables (e.g., u_k, J_{ij}, π, w_i) are convoluted with first derivatives of their variations. Consequently, integration-by-parts cannot reduce the maximum level of the temporal derivatives and we will require C^0 continuity of all variables in time. Note, however, that these variables are impulses of velocity, stress, pore pressure and relative fluid velocity, so that the continuity requirements only apply to these impulses. Thus, displacement and relative fluid displacement must be continuous in time, but the usual stress and pore pressure fields may be C^{-1} continuous (or discontinuous) in time.

On the other hand, the spatial derivatives in (12) are confined to terms involving variable pairs, including u_k - J_{ij}, u_k - π and π - w_i pairs. This means that there is an opportunity to reduce the continuity requirements on one variable in each pair. In order to best accomplish this objective, we must choose to perform spatial integration-by-parts to shift all derivatives from J_{ij}, δJ_{ij}, w_i and δw_i to the pair variable in each case. Then, u_k and π will require C^0 continuity in space, while J_{ij} and w_i will need to maintain only C^{-1} continuity. After performing all of these recommended integration-by-parts operations, the weak form becomes:

$$
\begin{aligned}
\delta I_{C_P} = & \int_\Omega \left[\delta \dot{u}_k * (1-n) \rho_s \dot{u}_k \right] d\Omega \\
& + \int_\Omega \left[\left(\delta \dot{u}_k + \frac{\delta \dot{w}_k}{n} \right) * n \rho_f \left(\dot{u}_k + \frac{\dot{w}_k}{n} \right) \right] d\Omega \\
& - \int_\Omega \left[\delta \dot{J}_{ij} * A_{ijkl} \dot{J}_{kl} \right] d\Omega \\
& - \int_\Omega \left[\delta \dot{\pi} * \frac{1}{Q} \dot{\pi} - \delta \breve{w}_i * \lambda_{ij} \breve{w}_j \right] d\Omega \\
& + \int_\Omega \left[\left(\delta \breve{J}_{ij} - \beta_{ij} \delta \breve{\pi} \right) * B_{ijk} \breve{u}_k \right] d\Omega \\
& + \int_\Omega \left[\left(\breve{J}_{ij} - \beta_{ij} \breve{\pi} \right) * B_{ijk} \delta \breve{u}_k \right] d\Omega \\
& + \int_\Omega \left[\delta \breve{w}_i * B_i \breve{\pi} + \breve{w}_i * B_i \delta \breve{\pi} \right] d\Omega \\
& - \int_\Omega \left[\delta \breve{u}_k * \breve{\bar{j}}_k \right] d\Omega + \int_\Omega \left[\delta \breve{\pi} * \breve{\bar{\Upsilon}} \right] d\Omega \\
& - \int_{\Gamma_t} \tfrac{1}{2} \left[\delta \breve{u}_k * \left(\breve{\bar{\tau}}_k + \breve{\tau}_k \right) \right] d\Gamma \\
& + \int_{\Gamma_v} \tfrac{1}{2} \left[\delta \breve{\tau}_k * \left(\breve{\bar{u}}_k - \breve{u}_k \right) \right] d\Gamma \\
& - \int_{\Gamma_q} \tfrac{1}{2} \left[\delta \breve{\pi} * \left(\breve{\bar{w}} + \breve{w} \right) \right] d\Gamma \\
& + \int_{\Gamma_p} \tfrac{1}{2} \left[\delta \breve{w} * \left(\breve{\bar{\pi}} - \breve{\pi} \right) \right] d\Gamma = 0
\end{aligned}
\tag{13}
$$

In the subsequent section, we will discuss the discretization of (13) and develop a time and space finite element method. Interestingly, for simple spatial and temporal variations, all of the integrals appearing in (13), including those involving fractional derivatives, can be evaluated in closed form.

However, before moving on to that discussion, let us recover the strong form of the problem by shifting all spatial and temporal derivatives from the variations (δu_k, δJ_{ij}, $\delta \pi$ and δw_i) to the real fields (u_k, J_{ij}, π and w_i) by using classical and fractional integration-by-parts for convolutions. All of the required formulas are defined in References [42, 43, 17], making this a systematic procedure. After some algebraic manipulation, the result can be written as follows:

$$
\begin{aligned}
\delta I_{C_P} = & \int_\Omega \delta u_k * \left[\begin{array}{l} \rho_o \ddot{u}_k + \rho_f \ddot{w}_k \\ \quad - B_{ijk}\left(\dot{J}_{ij} - \beta_{ij}\dot{\pi}\right) - \overline{f}_k \end{array} \right] d\Omega - \int_\Omega \delta J_{ij} * \left[A_{ijkl}\ddot{J}_{kl} - B_{ijk}\dot{u}_k \right] d\Omega \\
& - \int_\Omega \delta\pi * \left[\tfrac{1}{Q}\ddot{\pi} + B_i\dot{w}_i + \beta_{ij}B_{ijk}\dot{u}_k - \overline{\Gamma} \right] d\Omega + \int_\Omega \delta w_i * \left[\tfrac{\rho_f}{n}\ddot{w}_j + \rho_f\ddot{u}_j + \lambda_{ij}\dot{w}_i + B_j\dot{\pi} \right] d\Omega \\
& + \int_\Omega \delta u_k(t) \left[\begin{array}{l} \rho_o \dot{u}_k(0) + \rho_f \dot{w}_k(0) \\ \quad - B_{ijk}\left(J_{ij}(0) - \beta_{ij}\pi(0)\right) - \overline{j}_k(0) \end{array} \right] d\Omega - \int_\Omega \delta u_k(0)\left[\rho_o \dot{u}_k(t) + \rho_f \dot{w}_k(t)\right] d\Omega \\
& - \int_\Omega \delta J_{ij}(t)\left[A_{ijkl}\dot{J}_{kl}(0) - B_{ijk}u_k(0)\right] d\Omega + \int_\Omega \delta J_{ij}(0)\left[A_{ijkl}\dot{J}_{kl}(t)\right] d\Omega \\
& - \int_\Omega \delta\pi(t) \left[\begin{array}{l} \tfrac{1}{Q}\dot{\pi}(0) + B_i w_i(0) \\ \quad + \beta_{ij}B_{ijk}u_k(0) - \overline{\Upsilon}(0) \end{array} \right] d\Omega + \int_\Omega \delta\pi(0)\left[\tfrac{1}{Q}\dot{\pi}(t)\right] d\Omega \\
& + \int_\Omega \delta w_i(t) \left[\begin{array}{l} \tfrac{\rho_f}{n}\dot{w}_j(0) + \rho_f\dot{u}_j(0) \\ \quad + \lambda_{ij}w_i(0) + B_j\pi(0) \end{array} \right] d\Omega - \int_\Omega \delta w_i(0)\left[\tfrac{\rho_f}{n}\dot{w}_j(t) + \rho_f\dot{u}_j(t)\right] d\Omega \\
& + \int_{\Gamma_t} \tfrac{1}{2}\left[\delta u_k * t_k - \delta u_k * \overline{t}_k\right] d\Gamma + \int_{\Gamma_t} \tfrac{1}{2}\left[\delta u_k(t)\tau_k(0) - \delta u_k(t)\overline{\tau}_k(0)\right] d\Gamma \\
& + \int_{\Gamma_v} \tfrac{1}{2}\left[\delta u_k * t_k\right] d\Gamma + \int_{\Gamma_v} \tfrac{1}{2}\left[\delta u_k(t)\tau_k(0)\right] d\Gamma \\
& - \int_{\Gamma_v} \tfrac{1}{2}\left[\delta\tau_k * v_k - \delta\tau_k * \overline{v}_k\right] d\Gamma - \int_{\Gamma_v} \tfrac{1}{2}\left[\delta\tau_k(t)u_k(0) - \delta\tau_k(t)\overline{u}_k(0)\right] d\Gamma \\
& - \int_{\Gamma_\tau} \tfrac{1}{2}\left[\delta\tau_k * v_k\right] d\Gamma - \int_{\Gamma_\tau} \tfrac{1}{2}\left[\delta\tau_k(t)u_k(0)\right] d\Gamma \\
& + \int_{\Gamma_q} \tfrac{1}{2}\left[\delta\pi * q - \delta\pi * \overline{q}\right] d\Gamma + \int_{\Gamma_q} \tfrac{1}{2}\left[\delta\pi(t)w(0) - \delta\pi(t)\overline{w}(0)\right] d\Gamma \\
& + \int_{\Gamma_p} \tfrac{1}{2}\left[\delta\pi * q\right] d\Gamma - \int_{\Gamma_p} \tfrac{1}{2}\left[\delta\pi(t)w(0)\right] d\Gamma \\
& - \int_{\Gamma_p} \tfrac{1}{2}\left[\delta w * p - \delta w * \overline{p}\right] d\Gamma - \int_{\Gamma_p} \tfrac{1}{2}\left[\delta w(t)\pi(0) - \delta w(t)\overline{\pi}(0)\right] d\Gamma \\
& - \int_{\Gamma_q} \tfrac{1}{2}\left[\delta w * p\right] d\Gamma + \int_{\Gamma_q} \tfrac{1}{2}\left[\delta w(t)\pi(0)\right] d\Gamma = 0
\end{aligned}
\tag{14}
$$

again with $w = w_i n_i$, $q = q_i n_i$, $\tau_i = J_{ji} n_j$ and $t_i = \sigma_{ji} n_j$.

From (14) for arbitrary variations, we have as the Euler-Lagrange equations:

Governing partial differential equations

$$\rho_o \ddot{u}_k + \rho_f \ddot{w}_k - B_{ijk}\left(\dot{J}_{ij} - \beta_{ij}\dot{\pi}\right) = \overline{f}_k \tag{15a}$$

$$A_{ijkl}\ddot{J}_{kl} - B_{ijk}\dot{u}_k = 0 \tag{15b}$$

$$\frac{1}{Q}\ddot{\pi} + B_i\dot{w}_i + \beta_{ij}B_{ijk}\dot{u}_k = \overline{\Gamma} \tag{15c}$$

$$\frac{\rho_f}{n}\ddot{w}_j + \rho_f \ddot{u}_j + \lambda_{ij}\dot{w}_i + B_j\dot{\pi} = 0 \tag{15d}$$

for $x \in \Omega$, $\tau \in (0,t)$

Initial conditions over the spatial domain

$$\rho_o \dot{u}_k(0) + \rho_f \dot{w}_k(0) - B_{ijk}\left(J_{ij}(0) - \beta_{ij}\pi(0)\right) = \overline{j}_k(0) \tag{16a}$$

$$A_{ijkl}\dot{J}_{kl}(0) - B_{ijk}u_k(0) = 0 \tag{16b}$$

$$\frac{1}{Q}\dot{\pi}(0) + B_i w_i(0) + \beta_{ij}B_{ijk}u_k(0) = \overline{\Upsilon}(0) \tag{16c}$$

$$\frac{\rho_f}{n}\dot{w}_j(0) + \rho_f \dot{u}_j(0) + \lambda_{ij}w_i(0) + B_j\pi(0) = 0 \tag{16d}$$

for $x \in \Omega$

Boundary conditions over entire time span

$$t_k = \overline{t}_k \qquad x \in \Gamma_t \tag{17a}$$

$$v_k = \overline{v}_k \qquad x \in \Gamma_v \tag{17b}$$

$$q = \overline{q} \qquad x \in \Gamma_q \tag{17c}$$

$$p = \overline{p} \qquad x \in \Gamma_p \tag{17d}$$

for $\tau \in (0,t)$

Boundary conditions at time zero

$$\tau_k(0) = \overline{\tau}_k(0) \qquad x \in \Gamma_t \tag{18a}$$

$$u_k(0) = \overline{u}_k(0) \qquad x \in \Gamma_v \tag{18b}$$

$$w(0) = \overline{w}(0) \qquad x \in \Gamma_q \tag{18c}$$

$$\pi(0) = \overline{\pi}(0) \qquad x \in \Gamma_p \tag{18d}$$

In addition, the variations are constrained by the following:

Zero variations for specified boundary conditions

$$\delta\tau_k = 0 \qquad x \in \Gamma_t,\ \tau \in (0,t) \tag{19a}$$

$$\delta u_k = 0 \qquad x \in \Gamma_v,\ \tau \in (0,t) \tag{19b}$$

$$\delta w = 0 \qquad x \in \Gamma_q,\ \tau \in (0,t) \tag{19c}$$

$$\delta\pi = 0 \qquad x \in \Gamma_p,\ \tau \in (0,t) \tag{19d}$$

Zero end time variations for specified boundary conditions

$$\delta\tau_k(t) = 0 \qquad x \in \Gamma_t \tag{20a}$$

$$\delta u_k(t) = 0 \qquad x \in \Gamma_v \tag{20b}$$

$$\delta w(t) = 0 \qquad x \in \Gamma_q \tag{20c}$$

$$\delta\pi(t) = 0 \qquad x \in \Gamma_p \tag{20d}$$

Zero variations at initial time

$$\delta u_k(0) = 0 \tag{21a}$$

$$\delta J_{ij}(0) = 0 \tag{21b}$$

$$\delta\pi(0) = 0 \tag{21c}$$

$$\delta w_i(0) = 0 \tag{21d}$$

$$\text{for } x \in \Omega$$

This demonstrates that the Euler-Lagrange equations associated with the mixed convolved action, specified in (10), provide all of the relations that define the initial/boundary value problem of Biot dynamic poroelasticity.

As a result, we have now established a *Principle of Stationary Mixed Convolved Action* for a Linear Poroelastic Continuum undergoing infinitesimal deformation. This may be stated as follows: Of all the possible trajectories $\{u_k(\tau), J_{ij}(\tau), \pi(\tau), w_i(\tau)\}$ of the system during the time interval $(0,t)$, the one that renders the action I_{C_P} in (10) stationary, corresponds to the solution of the initial/boundary value problem. Thus, the stationary trajectory satisfies the balance laws of linear momentum (15a) and mass flow (15c), along with the linear elastic effective stress-strain constitutive relationship (15b) and the extended Darcy law (15d) in the domain Ω over the entire time interval. In addition, the traction (17a), velocity (17b), mass flux (17c) and pressure (17d) boundary conditions are satisfied throughout the time interval, while also complying with the initial conditions defined by (16a-d) in Ω and (18a-d) on the appropriate portions of the bounding surface. Furthermore, the possible trajectories under consideration during the variational process are constrained precisely by their need to satisfy the specified boundary and initial conditions of the problem in the form of (19a-d), (20a-d) and (21a-d).

Therefore, we are able to define a single real scalar functional, based upon convolution and fractional derivatives, which encapsulates all of the governing differential equations, along with the boundary and initial conditions, for linear dynamic poroelasticity. Furthermore, this represents the first true variational formulation for a dissipative poroelastic continuum.

We should note that the related frequency domain mixed convolution action principle can be found in the initial version of this MCA poroelastic research [44].

4 Space and Time Finite Element Formulation

In this section, we develop a computational formulation using finite elements for both space and time based on the weak form (13). Recall that in formulating (13), we chose to move all spatial derivatives onto the displacements u_i, pressure impulses π, and their corresponding variations, which was done to best reduce

the number of degrees of freedom in the final resulting system of equations. In the present work we will only deal with 2-d problems, however most of the equations either generally apply to 3-d problems also, or can be simply extended for 3-d analysis. Again, due to the appearance of first order spatial derivatives of displacements, pressure impulses, and the variations of these field variables in (13) we must enforce at least C^0 continuity in space for the quantities for a convergent formulation. However, for impulse of stress J_{ij} and fluid displacement w_i only C^{-1} continuity is necessary. This means that for the simplest case we can use linear spatial interpolation for displacements and pressure impulses, while we can consider the other quantities to be constant throughout the element and generally discontinuous across element boundaries. Temporally, first order derivatives appear for each field variable so we must maintain C^0 continuity in time, which for the simplest finite element scheme refers to using linear shape functions in time. Note that while the impulses of stress and fluid displacement must be continuous in time, generally the stresses and fluid velocities will not be.

Again we wish to emphasize the absence of the end time constraints that would appear in any application of Hamilton's principle. This allows for very natural use of temporal finite elements without needing to resort to any of the ad-hoc methods of dealing with this constraint [8, 45-47, 39-41, 36].

Upon spatial discretization of our domain and spatial integration we can the write the terms appearing in the weak form as

$$\int_{\Omega_e} \delta \dot{u}_k * \rho_o \dot{u}_k \, d\Omega = \delta \dot{\mathbf{u}}^T * \mathbf{M}_{uu} \, \dot{\mathbf{u}} \tag{22a}$$

$$\int_{\Omega_e} \delta \dot{J}_{ij} * A_{ijkl} \, \dot{J}_{kl} \, d\Omega = \delta \dot{\mathbf{J}}^T * \mathbf{A}_{JJ} \, \dot{\mathbf{J}} \tag{22b}$$

$$\int_{\Omega_e} \delta \breve{J}_{ij} * B_{ijk} \, \breve{u}_k \, d\Omega = \delta \breve{\mathbf{J}}^T * \mathbf{B}_{Ju} \, \breve{\mathbf{u}} \tag{22c}$$

$$\int_{\Omega_e} B_{ijk} \, \delta \breve{u}_k * \breve{J}_{ij} \, d\Omega = \delta \breve{\mathbf{u}}^T \, \mathbf{B}_{Ju}^T * \breve{\mathbf{J}} \tag{22d}$$

$$\int_{\Omega_e} \delta \breve{w}_i * \lambda_{ij} \breve{w}_j \, d\Omega = \delta \breve{\mathbf{w}}^T * \mathbf{\Lambda}_{ww} \breve{\mathbf{w}} \tag{22e}$$

$$\int_{\Omega_e} \delta \dot{w}_k * \frac{\rho_f}{n} \dot{w}_k \, d\Omega = \delta \dot{\mathbf{w}}^T * \mathbf{M}_{ww} \dot{\mathbf{w}} \tag{22f}$$

$$\int_{\Omega_e} \delta \dot{u}_k * \rho_f \dot{w}_k \, d\Omega = \delta \dot{\mathbf{u}}^T * \mathbf{M}_{uw} \dot{\mathbf{w}} \tag{22g}$$

$$\int_{\Omega_e} \delta \dot{\pi} * \frac{1}{Q} \dot{\pi} \, d\Omega = \delta \dot{\boldsymbol{\pi}}^T * \mathbf{A}_{\pi\pi} \dot{\boldsymbol{\pi}} \tag{22h}$$

$$\int_{\Omega_e} \beta_{ij} \delta \breve{\pi} * B_{ijk} \breve{u}_k \, d\Omega = \delta \breve{\boldsymbol{\pi}}^T * \mathbf{B}_{\pi u} \breve{\mathbf{u}} \tag{22i}$$

$$\int_{\Omega_e} B_i \delta \breve{\pi} * \breve{w}_i \, d\Omega = \delta \breve{\boldsymbol{\pi}}^T * \mathbf{B}_{\pi w} \breve{\mathbf{w}} \tag{22j}$$

where the bold face characters represent the spatially discretized counterpart of a variable. Here we wish to consider the simplest 2-d case where we use linear triangle elements for spatial interpolation of displacements and impulses of pressure. We then consider impulses of stress and fluid displacement to be constant throughout the element. The area shape functions can be written explicitly as

$$\boldsymbol{N}^T = \begin{pmatrix} 1 - \xi_1 - \xi_2 \\ \xi_1 \\ \xi_2 \end{pmatrix} \tag{23}$$

where ξ_i represent the local or natural element coordinates, which for the linear triangular elements are related to area coordinates. The shape functions, along with the Jacobian, are used to map our physical elements to the master isoparametric triangle element shown in Fig. 1, with ξ_1 and ξ_2 ranging from 0 to 1. Then we can represent the geometry of an element in terms of these local coordinates by interpolating the coordinates at nodes 1-3, such that

$$x = \boldsymbol{N}\, \boldsymbol{x} \tag{24a}$$

$$y = \boldsymbol{N}\, \boldsymbol{y} \tag{24a}$$

The components of the Jacobian matrix for an element are then defined as

$$J_{ij} \equiv \frac{\partial x_i}{\partial \xi_j} \tag{25}$$

such that

$$\boldsymbol{J} = \begin{pmatrix} \frac{\partial x}{\partial \xi_1} & \frac{\partial x}{\partial \xi_2} \\ \frac{\partial y}{\partial \xi_1} & \frac{\partial y}{\partial \xi_2} \end{pmatrix} \tag{26}$$

Then the area of an element, A, can be related to the determinant of the Jacobian by

$$A = |\boldsymbol{J}| / 2 \tag{27}$$

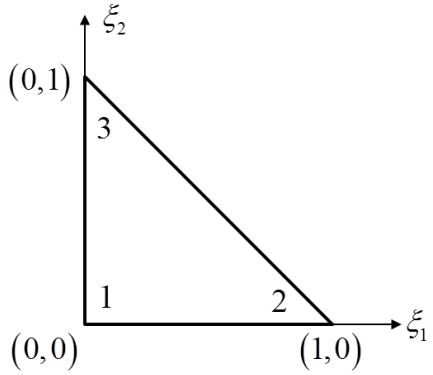

Fig. 1. Isoparametric master triangle element

Next we will define sub-matrices $\boldsymbol{b}_i$ as

$$\left(\boldsymbol{b}_{Ju}\right)_i = \begin{pmatrix} \frac{dN_i}{dx} & 0 \\ 0 & \frac{dN_i}{dy} \\ \frac{dN_i}{dy} & \frac{dN_i}{dx} \end{pmatrix} \tag{28a}$$

$$(\boldsymbol{b}_{\pi u})_i = (\boldsymbol{b}_{\pi w})_i = \begin{pmatrix} \frac{dN_i}{dx} & \frac{dN_i}{dy} \end{pmatrix} \tag{28b}$$

Then the full $\boldsymbol{b}$ matrices can be written by concatenating the sub-matrices such that

$$\boldsymbol{b}_{Ju} = \begin{pmatrix} \boldsymbol{b}_{Ju1} & \boldsymbol{b}_{Ju2} & \boldsymbol{b}_{Ju3} \end{pmatrix} \tag{29a}$$

$$\boldsymbol{b}_{\pi u} = \begin{pmatrix} \boldsymbol{b}_{\pi u1} & \boldsymbol{b}_{\pi u2} & \boldsymbol{b}_{\pi u3} \end{pmatrix} \tag{29b}$$

$$\boldsymbol{b}_{\pi w} = \begin{pmatrix} \boldsymbol{b}_{\pi w1} \\ \boldsymbol{b}_{\pi w1} \\ \boldsymbol{b}_{\pi w1} \end{pmatrix} \tag{29c}$$

and finally we can the relate these $\boldsymbol{b}$ matrices to the $\mathbf{B}$ matrices appearing in our finite element formulation by

$$\mathbf{B}_{Ju} = \int_{\Omega_e} \boldsymbol{b}_{Ju}\, d\Omega \tag{30a}$$

$$\mathbf{B}_{\pi w} = \int_{\Omega_e} \boldsymbol{b}_{\pi w}\, d\Omega \tag{30b}$$

$$\mathbf{B}_{\pi u} = \int_{\Omega e} \beta\, \boldsymbol{N}^T \boldsymbol{b}_{\pi u}\, d\Omega \tag{30c}$$

where all integration is carried out numerically via Gauss quadrature. For more information on shape functions, mapped elements, and numerical integration the reader is referred to the standard finite element textbooks [48, 49]. For an isotropic material the other matrices in equations (22) can be computed as

$$\mathbf{A}_{JJ} = \frac{1+\nu}{E} A\, h \begin{bmatrix} 1-\nu & -\nu & 0 \\ -\nu & 1-\nu & 0 \\ 0 & 0 & 2 \end{bmatrix} \qquad \text{for plane strain} \tag{31a}$$

$$\mathbf{A}_{JJ} = \frac{1}{E} A\, h \begin{bmatrix} 1 & -\nu & 0 \\ -\nu & 1 & 0 \\ 0 & 0 & 2(1+\nu) \end{bmatrix} \qquad \text{for plane stress} \tag{31b}$$

$$\mathbf{A}_{\pi\pi} = \frac{1}{Q} A\, h\, \mathbf{I}_3 \tag{31c}$$

$$\mathbf{\Lambda}_{ww} = \lambda\, A\, h\, \mathbf{I}_3 \tag{31d}$$

where $\mathbf{I}_n$ is an $[n \times n]$ identity matrix, h is the element thickness, Q is the Biot parameter, λ is the inverse of the isotropic permeability κ, ν is Poisson's ratio, and E is Young's modulus.

For the $\mathbf{M}$ matrices we use lumped mass representations such that we have

$$\mathbf{M}_{uu} = \rho_o \; A\, h\, \mathbf{I}_6 / 3 \tag{32a}$$

$$\mathbf{M}_{ww} = \frac{\rho_f}{n} A\, h\, \mathbf{I}_2 \tag{32b}$$

$$\mathbf{M}_{uw} = \frac{1}{3} A h \rho_f \begin{pmatrix} 1 & 0 & 1 & 0 & 1 & 0 \\ 0 & 1 & 0 & 1 & 0 & 1 \end{pmatrix}^T \tag{32c}$$

However it would of course be just as simple to use linear interpolation to calculate these $\mathbf{M}$ matrices. For example, for the coupling mass terms we would have

$$\mathbf{M}_{uw} = \int_{\Omega_e} \boldsymbol{h}^T \; \rho_f \; d\Omega \tag{33}$$

where

$$\boldsymbol{h}_i = \begin{pmatrix} N_i & 0 \\ 0 & N_i \end{pmatrix} \tag{34a}$$

$$\boldsymbol{h} = \begin{pmatrix} \boldsymbol{h}_1 & \boldsymbol{h}_2 & \boldsymbol{h}_3 \end{pmatrix} \tag{34b}$$

In a similar manner to the other terms appearing in the weak form (13), after spatial discretization, the body force contributions over an element become:

$$\int_{\Omega_e} \delta \breve{u}_k * \breve{\bar{j}}_k \; d\Omega = \delta \breve{\mathbf{u}}^T * \breve{\bar{\mathbf{j}}} \tag{35}$$

while the terms from the boundary conditions can be obtained by integration over an element edge, yielding

$$\int_{\Gamma_t} \tfrac{1}{2} \left[\delta \breve{u}_k * \left(\breve{\bar{\tau}}_k + \breve{\tau}_k \right) \right] d\Gamma = \tfrac{1}{2} \delta \breve{\mathbf{u}}^T * \left(\breve{\bar{\boldsymbol{\tau}}} + \breve{\boldsymbol{\tau}} \right) \tag{36a}$$

$$\int_{\Gamma_v} \tfrac{1}{2} \left[\delta \breve{\tau}_k * \left(\breve{\bar{u}}_k - \breve{u}_k \right) \right] d\Gamma = \tfrac{1}{2} \delta \breve{\boldsymbol{\tau}}^T * \left(\breve{\bar{\mathbf{u}}} - \breve{\mathbf{u}} \right) \tag{36b}$$

Although for higher order elements there are some interesting ways to accommodate the influences defined in (36a,b), here we simply equate the unknown variables to the known values (i.e., $\breve{\boldsymbol{\tau}} = \breve{\bar{\boldsymbol{\tau}}}$ and $\breve{\mathbf{u}} = \breve{\bar{\mathbf{u}}}$) on edges associated with Γ_t and Γ_v, such that the enforced tractions have a contribution defined by

$$\int_{\Gamma_t} \tfrac{1}{2}\left[\delta\breve{u}_k * \left(\breve{\bar{\tau}}_k + \breve{\tau}_k \right) \right] d\Gamma = \delta\breve{\mathbf{u}}^T * \breve{\bar{\boldsymbol{\tau}}} \tag{37a}$$

while the enforced displacement integral has no explicit additional effect, because

$$\int_{\Gamma_v} \tfrac{1}{2}\left[\delta\breve{\tau}_k * \left(\breve{\bar{u}}_k - \breve{u}_k \right) \right] d\Gamma = 0 \tag{37b}$$

Similarly, for the hydraulic terms, after spatial discretization, the body source contributions over an element can be written:

$$\int_{\Omega_e} \delta\breve{\pi} * \breve{\bar{\Upsilon}}\, d\Omega = \delta\breve{\boldsymbol{\pi}}^T * \breve{\bar{\boldsymbol{\Upsilon}}} \tag{38}$$

while the terms from the boundary conditions can be evaluated through integration over an element edge, thus yielding

$$\int_{\Gamma_q} \tfrac{1}{2}\left[\delta\breve{\pi} * \left(\breve{\bar{w}} + \breve{w} \right) \right] d\Gamma = \tfrac{1}{2}\delta\breve{\boldsymbol{\pi}}^T * \left(\breve{\bar{\mathbf{w}}} + \breve{\mathbf{w}} \right) \tag{39a}$$

$$\int_{\Gamma_p} \tfrac{1}{2}\left[\delta\breve{w} * \left(\breve{\bar{\pi}} - \breve{\pi} \right) \right] d\Gamma = \tfrac{1}{2}\delta\breve{\mathbf{w}}^T * \left(\breve{\bar{\boldsymbol{\pi}}} - \breve{\boldsymbol{\pi}} \right) \tag{39b}$$

similar to the elastic boundary condition terms, we simply equate the unknown variables to the known values (i.e., $\breve{\mathbf{w}} = \breve{\bar{\mathbf{w}}}$ and $\breve{\boldsymbol{\pi}} = \breve{\bar{\boldsymbol{\pi}}}$) on edges associated with Γ_q and Γ_p, such that the enforced fluid displacements have a contribution defined by

$$\int_{\Gamma_q} \tfrac{1}{2}\left[\delta\breve{\pi} * \left(\breve{\bar{w}} + \breve{w} \right) \right] d\Gamma = \delta\breve{\boldsymbol{\pi}}^T * \breve{\bar{\mathbf{w}}} \tag{40a}$$

while the enforced pressure impulse integral has no explicit additional effect, because

$$\int_{\Gamma_p} \tfrac{1}{2}\left[\delta\breve{w} * \left(\breve{\bar{\pi}} - \breve{\pi} \right) \right] d\Gamma = 0 \tag{40b}$$

Substituting the preceding discretized representations into equation (13) provides the spatially discretized mixed weak form for an element, which can be written:

$$
\begin{aligned}
&\delta\dot{\mathbf{u}}^T * \mathbf{M}_{uu}\,\dot{\mathbf{u}} - \delta\dot{\mathbf{J}}^T * \mathbf{A}_{JJ}\,\dot{\mathbf{J}} + \delta\breve{\mathbf{J}}^T * \mathbf{B}_{Ju}\,\breve{\mathbf{u}} + \delta\breve{\mathbf{u}}^T\,\mathbf{B}_{Ju}^T * \breve{\mathbf{J}} \\
&\quad + \delta\dot{\mathbf{w}}^T * \mathbf{M}_{ww}\dot{\mathbf{w}} + \delta\breve{\mathbf{w}}^T * \mathbf{\Lambda}_{ww}\breve{\mathbf{w}} - \delta\dot{\boldsymbol{\pi}}^T * \mathbf{A}_{\pi\pi}\dot{\boldsymbol{\pi}} \\
&\quad + \delta\dot{\mathbf{u}}^T * \mathbf{M}_{uw}\dot{\mathbf{w}} + \delta\dot{\mathbf{w}}^T\,\mathbf{M}_{uw}^T * \dot{\mathbf{u}} \\
&\quad + \delta\breve{\boldsymbol{\pi}}^T * \mathbf{B}_{\pi w}\breve{\mathbf{w}} + \delta\breve{\mathbf{w}}^T\,\mathbf{B}_{\pi w}^T * \breve{\boldsymbol{\pi}} \\
&\quad - \delta\breve{\boldsymbol{\pi}}^T * \mathbf{B}_{\pi u}\breve{\mathbf{u}} - \delta\breve{\mathbf{u}}^T\,\mathbf{B}_{\pi u}^T * \breve{\boldsymbol{\pi}} \\
&\quad - \delta\breve{\mathbf{u}}^T * \breve{\breve{\mathbf{j}}} - \delta\breve{\mathbf{u}}^T * \breve{\breve{\boldsymbol{\tau}}} + \delta\breve{\boldsymbol{\pi}}^T * \breve{\breve{\boldsymbol{\Upsilon}}} - \delta\breve{\boldsymbol{\pi}}^T * \breve{\breve{\mathbf{w}}} = 0
\end{aligned}
\tag{41}
$$

Next we must consider temporal discretization of the weak form. As previously mentioned, due to the presence of first derivatives we must maintain at least C^0 continuity of our field variables, thus linear shape functions are used for temporal interpolation. Then, over a time interval from $0 \le t \le \Delta t$, we have:

$$\mathbf{u}(t) = \mathbf{u}_0 N_0(t) + \mathbf{u}_1 N_1(t) \tag{42a}$$

$$\mathbf{J}(t) = \mathbf{J}_0 N_0(t) + \mathbf{J}_1 N_1(t) \tag{42b}$$

$$\boldsymbol{\pi}(t) = \boldsymbol{\pi}_0 N_0(t) + \boldsymbol{\pi}_1 N_1(t) \tag{42c}$$

$$\mathbf{w}(t) = \mathbf{w}_0 N_0(t) + \mathbf{w}_1 N_1(t) \tag{42d}$$

in terms of the temporal shape functions

$$N_0(t) = 1 - \tfrac{t}{\Delta t}; \quad N_1(t) = \tfrac{t}{\Delta t} \tag{43a,b}$$

with similar temporal interpolation for the variations of our field variables, as well as applied body force, traction, body source, and fluid displacement terms.

We now substitute the temporally discretized variables (42a-d) into equation (41), perform all necessary convolution integrals in closed form, set all variations at $t = 0$ to zero, while allowing the variations at $t = \Delta t$ to remain arbitrary, multiply through by $4/\Delta t$, and collect like terms to arrive at the following symmetric set of linear algebraic equations:

$$\frac{4}{(\Delta t)^2}\begin{bmatrix} \mathbf{M}_{uu} & \frac{\Delta t}{2}\mathbf{B}_{Ju}^T & \mathbf{M}_{uw} & -\frac{\Delta t}{2}\mathbf{B}_{\pi u}^T \\ \frac{\Delta t}{2}\mathbf{B}_{Ju} & -\mathbf{A}_{JJ} & 0 & 0 \\ \mathbf{M}_{uw}^T & 0 & \mathbf{M}_{ww}+\frac{\Delta t}{2}\mathbf{\Lambda}_{ww} & \frac{\Delta t}{2}\mathbf{B}_{\pi w}^T \\ -\frac{\Delta t}{2}\mathbf{B}_{\pi u} & 0 & \frac{\Delta t}{2}\mathbf{B}_{\pi w} & -\mathbf{A}_{\pi\pi} \end{bmatrix}\begin{Bmatrix} \mathbf{u}_1 \\ \mathbf{J}_1 \\ \mathbf{w}_1 \\ \boldsymbol{\pi}_1 \end{Bmatrix}$$
$$= \frac{2}{\Delta t}\begin{Bmatrix} \mathbf{j}_1+\mathbf{j}_0 \\ \mathbf{0} \\ \mathbf{0} \\ \boldsymbol{\Upsilon}_1+\boldsymbol{\Upsilon}_0 \end{Bmatrix} + \frac{4}{(\Delta t)^2}\begin{bmatrix} \mathbf{M}_{uu} & -\frac{\Delta t}{2}\mathbf{B}_{Ju}^T & \mathbf{M}_{uw} & \frac{\Delta t}{2}\mathbf{B}_{\pi u}^T \\ -\frac{\Delta t}{2}\mathbf{B}_{Ju} & -\mathbf{A}_{JJ} & 0 & 0 \\ \mathbf{M}_{uw}^T & 0 & \mathbf{M}_{ww}-\frac{\Delta t}{2}\mathbf{\Lambda}_{ww} & -\frac{\Delta t}{2}\mathbf{B}_{\pi w}^T \\ \frac{\Delta t}{2}\mathbf{B}_{\pi u} & 0 & -\frac{\Delta t}{2}\mathbf{B}_{\pi w} & -\mathbf{A}_{\pi\pi} \end{bmatrix}\begin{Bmatrix} \mathbf{u}_0 \\ \mathbf{J}_0 \\ \mathbf{w}_0 \\ \boldsymbol{\pi}_0 \end{Bmatrix} \tag{44}$$

where

$$\mathbf{M}_{ww1} = \mathbf{M}_{ww} + \tfrac{\Delta t}{2}\mathbf{\Lambda}_{ww} \tag{45a}$$

$$\mathbf{M}_{ww0} = \mathbf{M}_{ww} - \tfrac{\Delta t}{2}\mathbf{\Lambda}_{ww} \tag{45b}$$

We are free to use (44) as our final set of equations, however there is one more simplification that can be made. Because we chose to interpolate the impulses of stress and fluid displacements as element-by-element C^{-1} functions, we have the freedom to condense these variables out at the element level prior to solving (44), which can save considerable computation time. Then solving (44) for $\mathbf{J}_1$ and $\mathbf{w}_1$ gives us

$$\mathbf{J}_1 = \mathbf{A}_{JJ}^{-1}\left[\tfrac{\Delta t}{2}\mathbf{B}_{Ju}\left(\mathbf{u}_1+\mathbf{u}_0\right)+\mathbf{A}_{JJ}\mathbf{J}_0\right] \tag{46a}$$

$$\mathbf{w}_1 = \mathbf{M}_{ww1}^{-1}\left[\mathbf{M}_{uw}^T\left(\mathbf{u}_0-\mathbf{u}_1\right)-\tfrac{\Delta t}{2}\mathbf{B}_{\pi w}^T\left(\boldsymbol{\pi}_0+\boldsymbol{\pi}_1\right)+\mathbf{M}_{ww0}\mathbf{w}_0\right] \tag{46b}$$

and after substituting these relations into (44) and rearranging we can write the condensed set of equations as

$$\begin{bmatrix} \mathbf{K}_{uu1}^e & \mathbf{K}_{u\pi 1}^e \\ \mathbf{K}_{\pi u1}^e & \mathbf{K}_{\pi\pi 1}^e \end{bmatrix}\begin{Bmatrix} \mathbf{u}_1 \\ \boldsymbol{\pi}_1 \end{Bmatrix} = \begin{Bmatrix} \mathbf{f}_{u1}^e \\ \mathbf{f}_{\pi 1}^e \end{Bmatrix} \tag{47}$$

where

$$\mathbf{K}_{uu1}^e = \mathbf{B}_{Ju}^T\,\mathbf{A}_{JJ}^{-1}\,\mathbf{B}_{Ju} + \tfrac{4}{(\Delta t)^2}\mathbf{M}_{uu} - \tfrac{4}{(\Delta t)^2}\mathbf{M}_{uw}\mathbf{M}_{ww1}^{-1}\mathbf{M}_{uw}^T \tag{48a}$$

$$\mathbf{K}_{\pi\pi 1}^e = -\mathbf{B}_{\pi w}\mathbf{M}_{ww1}^{-1}\mathbf{B}_{\pi w}^T - \tfrac{4}{(\Delta t)^2}\mathbf{A}_{\pi\pi} \tag{48b}$$

$$\mathbf{K}^{e}_{u\pi 1} = \mathbf{K}^{e}_{u\pi 0} = \mathbf{K}^{e\,T}_{\pi u 1} = -\tfrac{2}{\Delta t}\left(\mathbf{M}_{uw}\mathbf{M}^{-1}_{ww1}\mathbf{B}^{T}_{\pi w} + \mathbf{B}^{T}_{\pi u}\right) \tag{48c}$$

$$\mathbf{f}^{e}_{u1} = \tfrac{2}{\Delta t}\left(\mathbf{j}_1 + \mathbf{j}_0\right) - \mathbf{K}^{e}_{uu0}\,\mathbf{u}_0 - \mathbf{K}^{e}_{u\pi 0}\,\boldsymbol{\pi}_0 - \tfrac{4}{\Delta t}\mathbf{B}^{T}_{Ju}\,\mathbf{J}_0 - \tfrac{4}{(\Delta t)^2}\left(\mathbf{M}_{uw}\mathbf{M}^{-1}_{ww1}\mathbf{M}_{ww0} - \mathbf{M}_{uw}\right)\mathbf{w}_0 \tag{49a}$$

$$\mathbf{f}^{e}_{\pi 1} = \tfrac{2}{\Delta t}\left(\boldsymbol{\Upsilon}_1 + \boldsymbol{\Upsilon}_0\right) - \mathbf{K}^{e}_{\pi\pi 0}\,\boldsymbol{\pi}_0 - \mathbf{K}^{e}_{\pi u 0}\,\mathbf{u}_0 - \tfrac{4}{\Delta t}\mathbf{B}_{\pi w 0}\mathbf{w}_0 \tag{49b}$$

and

$$\mathbf{K}^{e}_{uu0} = \mathbf{B}^{T}_{Ju}\,\mathbf{A}^{-1}_{JJ}\,\mathbf{B}_{Ju} - \tfrac{4}{(\Delta t)^2}\mathbf{M}_{uu} + \tfrac{4}{(\Delta t)^2}\mathbf{M}_{uw}\mathbf{M}^{-1}_{ww1}\mathbf{M}^{T}_{uw} \tag{50a}$$

$$\mathbf{K}^{e}_{\pi\pi 0} = -\,\mathbf{B}_{\pi w}\mathbf{M}^{-1}_{ww1}\,\mathbf{B}^{T}_{\pi w} + \tfrac{4}{(\Delta t)^2}\mathbf{A}_{\pi\pi} \tag{50b}$$

$$\mathbf{K}^{e\,T}_{\pi u 0} = \tfrac{2}{\Delta t}\left(\mathbf{M}_{uw}\mathbf{M}^{-1}_{ww1}\mathbf{B}^{T}_{\pi w} - \mathbf{B}^{T}_{\pi u}\right) \tag{50c}$$

$$\mathbf{B}_{\pi w 0} = \tfrac{1}{2}\left(\mathbf{B}_{\pi w}\mathbf{M}^{-1}_{ww1}\mathbf{M}_{ww0} + \mathbf{B}_{\pi w}\right) \tag{51}$$

$$\mathbf{M}_{uw0} = \left(\mathbf{M}_{uw}\mathbf{M}^{-1}_{ww1}\mathbf{M}_{ww0} - \mathbf{M}_{uw}\right) \tag{52}$$

While all of this has been formulated on the element level, in practice we actually wish to solve the following global set of equations that can be arrived at via standard assembly procedures [48, 49]:

$$\begin{bmatrix} \mathbf{K}_{uu1} & \mathbf{K}_{u\pi 1} \\ \mathbf{K}_{\pi u 1} & \mathbf{K}_{\pi\pi 1} \end{bmatrix} \begin{Bmatrix} \mathbf{u}_n \\ \boldsymbol{\pi}_n \end{Bmatrix} = \begin{Bmatrix} \mathbf{f}_{un} \\ \mathbf{f}_{\pi n} \end{Bmatrix} \tag{53}$$

where $\mathbf{u}_n$ and $\boldsymbol{\pi}_n$ consist of all nodal displacements and pressure impulses, respectively, at each time step n. Then one simply needs to first compute the global stiffness $\mathbf{K}$ matrices, specify known initial conditions, and then march the solution in time by computing the right hand side at each time step and solving (53).

5 Dynamic Poroelasticity Problems

In this section, the mixed convolved action finite element formulation is applied to a couple of two-dimensional problems of dynamic poroelasticity. For the first example, the MCA results are compared with

a boundary element solution [50], while a time step study is performed for the second example to demonstrate the convergence characteristics of the present development.

5.1 Dynamic poroelastic half-space subject to traction pulses

For this problem we consider the dynamic response of a poroelastic half-space to a spatially uniform normal traction pulse applied to the free surface at $x = 0$. Figure 2 illustrates a problem schematic, while Fig. 3 shows the actual domain used for analysis. This domain is then split into 1260 triangular elements with biased refinement towards the free surface. Elements have approximate edge length of 0.02 close to the free surface and 0.2 near to the fixed right side boundary. Here we consider all material parameters to be non-dimensional, with $\rho_o = 1$, $\lambda = 1$, $E = 0.316$, $\nu = 0.2$, $\rho_f = 0.973$, $Q = 1.459$, $\beta = 0.667$, and $n = 0.333$.

For elastic boundary conditions we consider all surfaces to be on smooth rollers, except the free surface $x = 0$, where a single normal traction pulse is applied. This pulse is spatially constant but for case one is a half-sine pulse in time such that $\bar{t}_x(t) = \sin(\pi t)$ for $0 \le t \le 1$, and for case two is a sine-squared pulse in time such that $\bar{t}_x = \sin^2(\pi t)$ for $0 \le t \le 1$. The remaining boundary conditions are zero fluid displacement for all surfaces except the free surface, where we have the pressure free condition $\bar{p} = 0$. For all simulations a time step of $\Delta t = 0.01$ is used.

In Figs. 4a and 4b we plot pore pressure p and horizontal displacement u_x at two points, both located at $x = 1$ but having different vertical positions, versus time, respectively, for the half-sine pulse loading. The results for these two points are essentially identical, as should be expected for this 1-d problem. Meanwhile, in Figs. 5a and 5b we plot p and u_x at the same point located at $x = 1$ versus time, respectively, for the

sine-squared pulse loading. For all plots we compare the MCA solutions to the analytical solutions presented in Ref. [51].

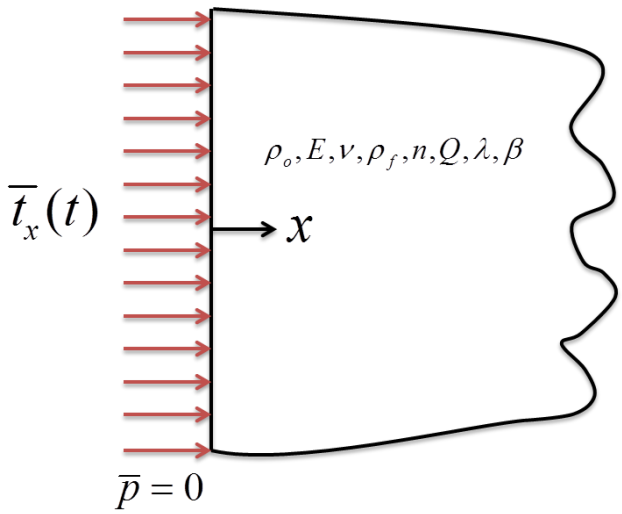

Fig. 2. Poroelastic half-space with applied surface traction pulse

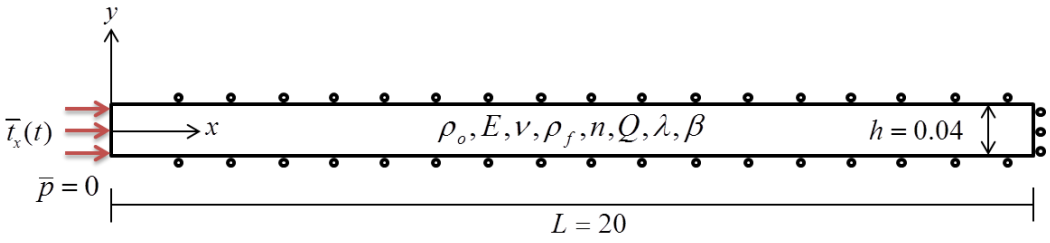

Fig. 3. Poroelastic half-space solution domain and boundary conditions

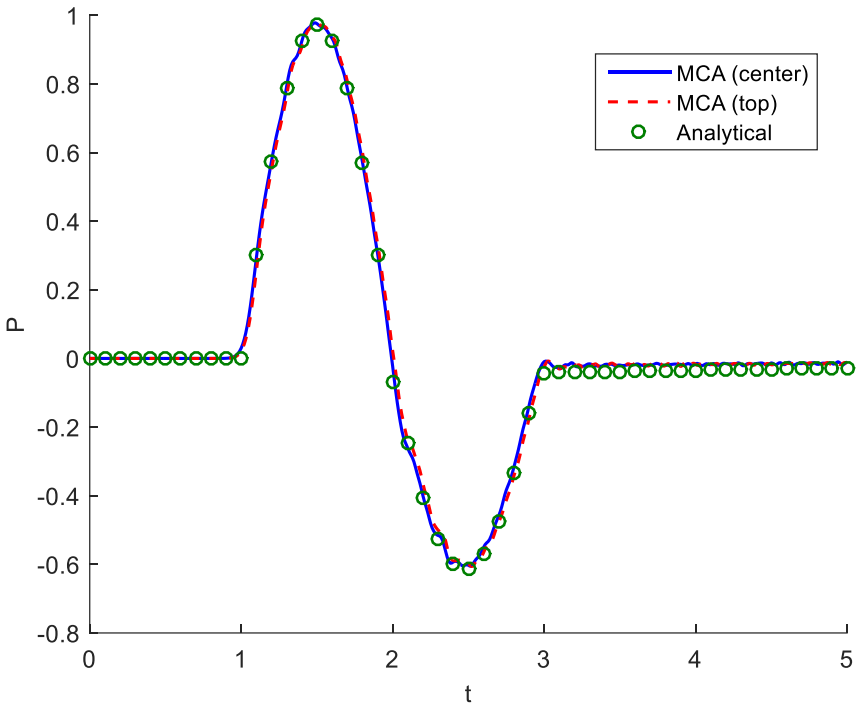

Fig. 4a. Pore pressure at $x = 1$ versus time for half-sine pulse

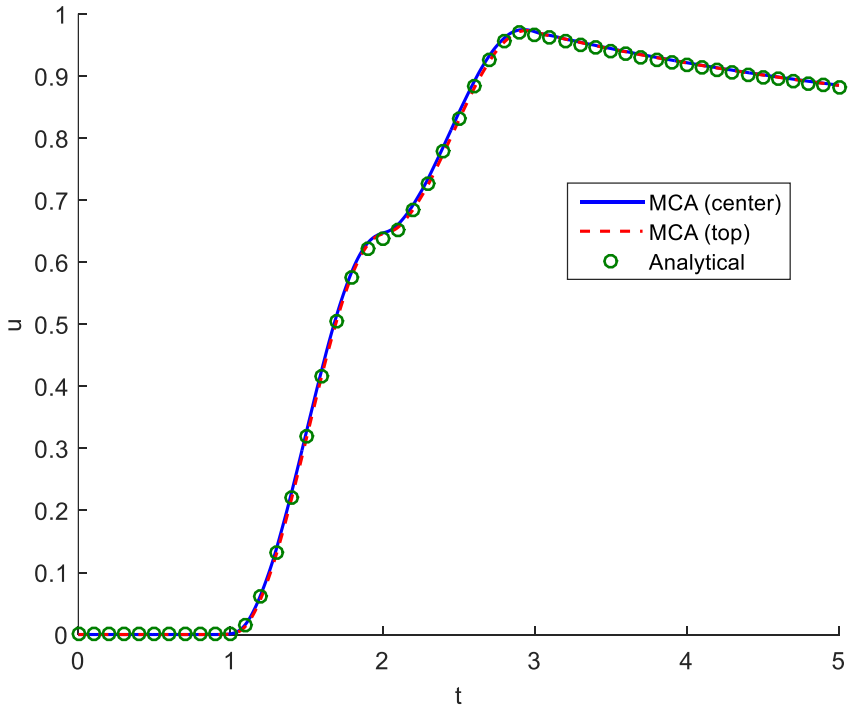

Fig. 4b. Horizontal displacement at $x = 1$ versuss time for half-sine pulse

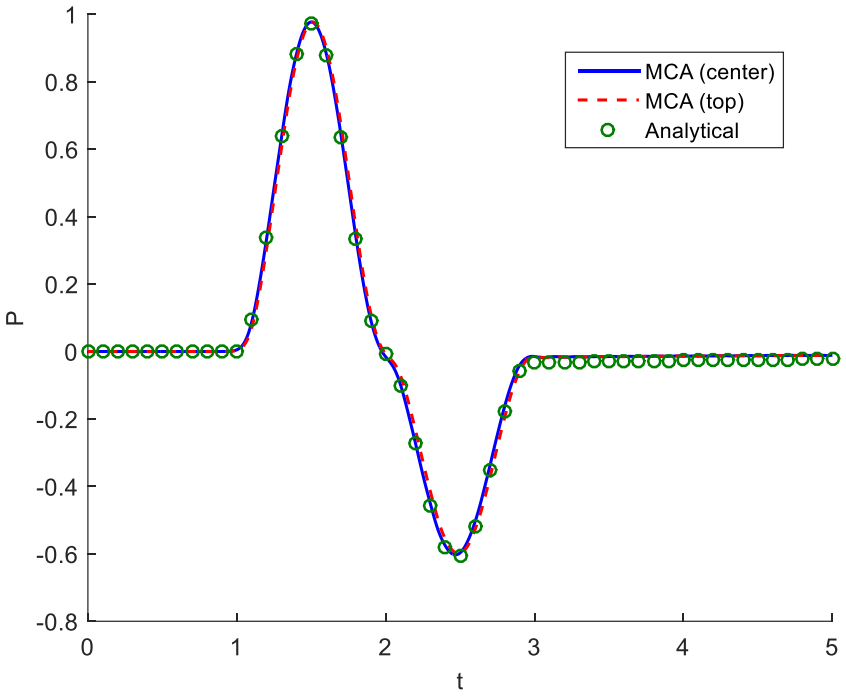

Fig. 5a. Pore pressure at $x = 1$ versus time for sine-squared pulse

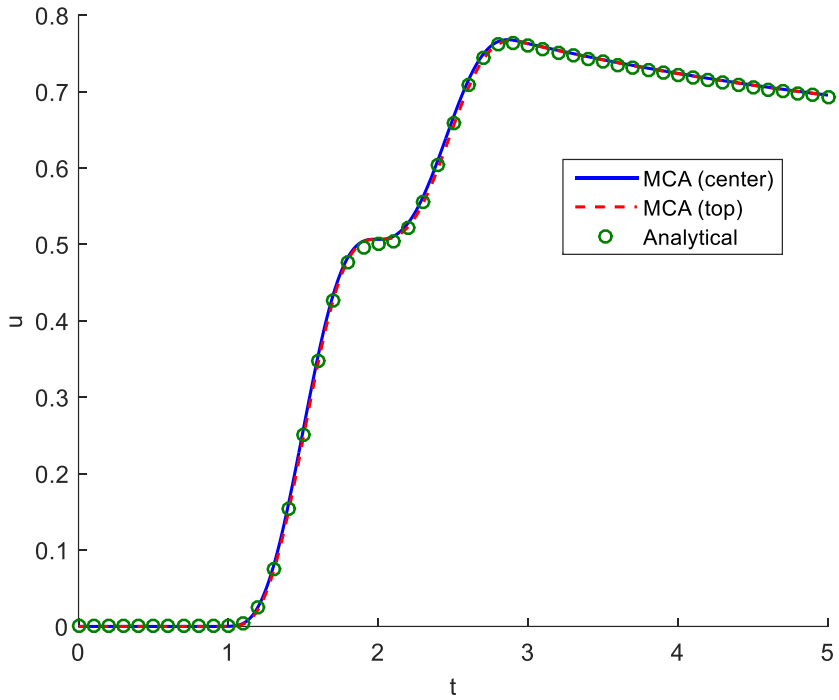

Fig. 5b. Horizontal displacement at $x = 1$ versus time for sine-squared pulse

5.2 Explosion in a cylindrical cavity beneath the surface of a half-space

This second problem examines the dynamic poroelastic response resulting from a radial stress pulse supplied to the surface of a cylindrical cavity embedded in a half-space, as shown in Fig. 6. The cavity is positioned at a depth of $H = 2$ below the free surface $y = 0$ and has diameter $D = 1$, where again all parameters are nondimensional. This is shown in Fig. 7, which provides the actual mesh consisting of 1136 triangular elements used for analysis. Elements have approximate edge length of 0.1 surrounding the cavity, and approximate edge length of 1 on the surfaces furthest from the cavity. The boundaries to the right and bottom of the cavity are far enough away such that waves never reach these distances for the time duration of our simulations, and hence despite the fixed boundary conditions on these surface we still have the equivalent of a half-space.

The explosion pulse is modelled as a radially uniform applied traction $\bar{t}_r(t)$ having unit amplitude and a sine-squared temporal profile with unit duration, such that for a single pulse we have $\bar{t}_r(t) = \sin^2(\pi t)$ for $0 \le t \le 1$. Then we also have two cases for hydraulic boundary conditions for the cavity. For the first case we consider the cavity to be impermeable such that $\bar{w} = 0$ and for the second we consider a permeable cavity such that $\bar{p} = 0$. Then for other boundary conditions we consider the free surface to be traction free and permeable such that $\bar{t}_x = \bar{t}_x = \bar{p} = 0$, and all other surface are on smooth rollers and impermeable, such that there is zero normal displacements and $\bar{w} = 0$. For material parameters, we use the following values: $\rho_o = 1$, $\lambda = 1$, $E = 1$, $\nu = 0$, $\rho_f = 3/4$, $Q = 3/2$, $\beta = 3/4$, and $n = 1/4$.

In Fig. 8, the time history of the pore pressure response at point A is provided for the impermeable case for several different time step sizes. Convergence is demonstrated clearly as the time step is reduced to a duration of $\Delta t = 0.01$, which is then selected for all subsequent analyses for this problem.

Next, Fig. 9 shows the pore pressure p at point A plotted over an extended period of time. Meanwhile, in Fig. 10, the vertical displacements u_y at point O located on the free surface above the cavity and at point A on the top surface of the cavity are plotted against time. Both Figs. 9 and 10 are for the impermeable cavity boundary condition case. Finally, Fig. 11 presents the vertical displacements plotted against time, but for the permeable cavity boundary condition. Interestingly the maximum displacement peak on the surface of the cavity is slightly larger than on the free surface for the permeable condition, while the maximum displacement peak on the free surface at point O is slightly larger for the impermeable case.

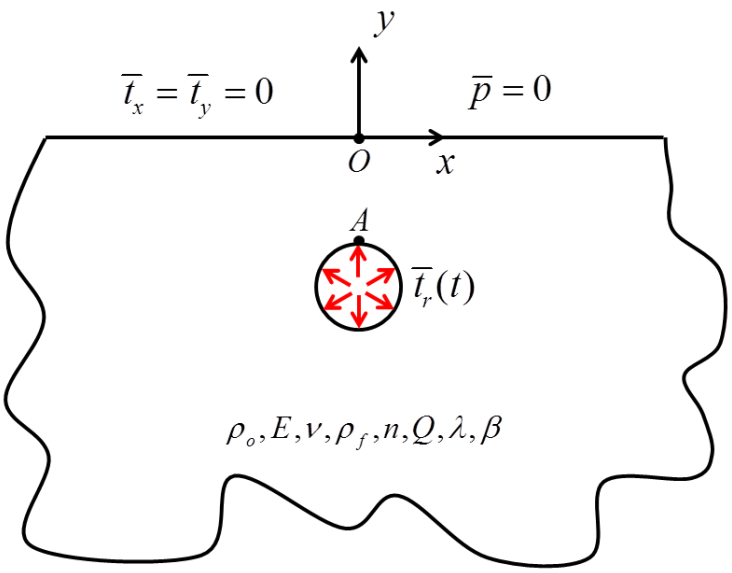

Fig. 6. Explosion in a cylindrical cavity problem schematic

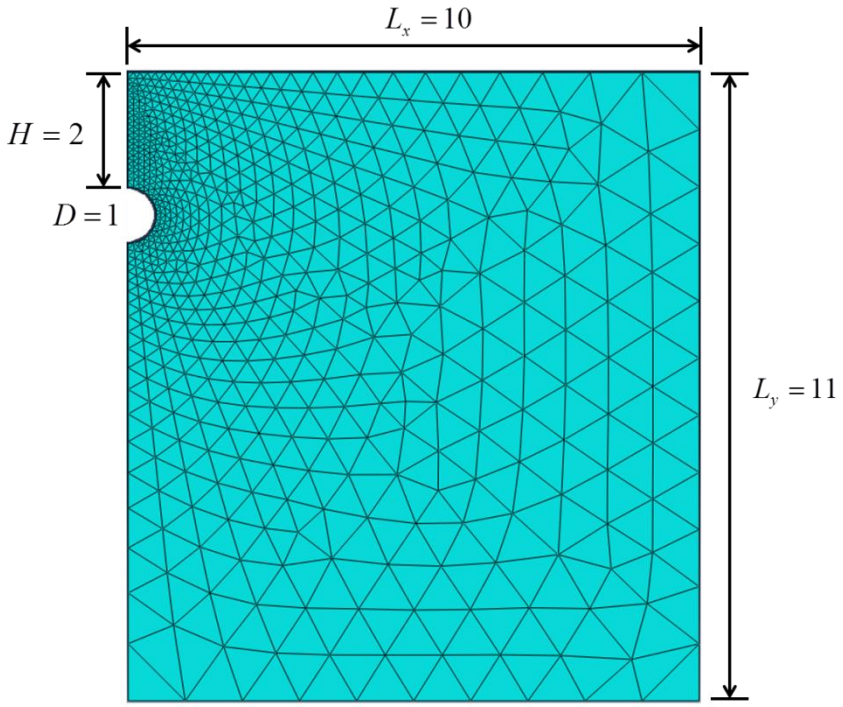

Fig. 7. Explosion in a cylindrical cavity mesh

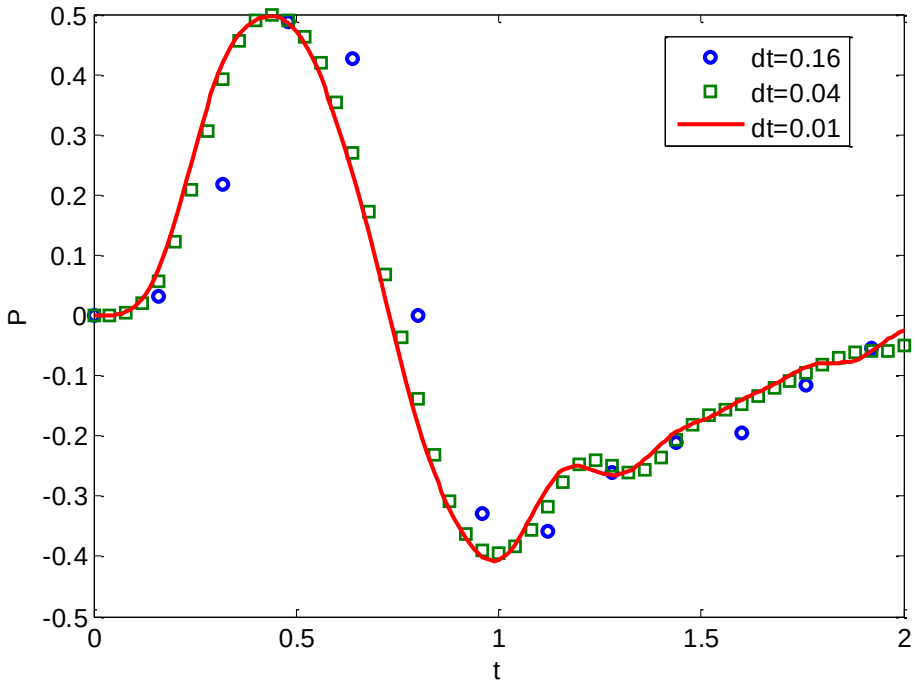

Fig. 8. Convergence study for pore pressure at point A versus time, impermeable cavity

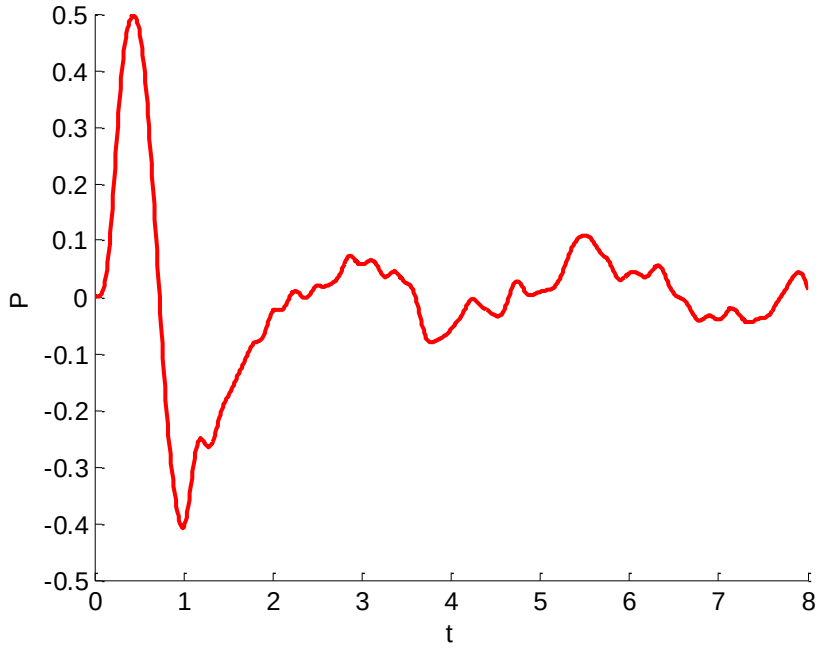

Fig. 9. Pore pressure at point A versus time, impermeable cavity

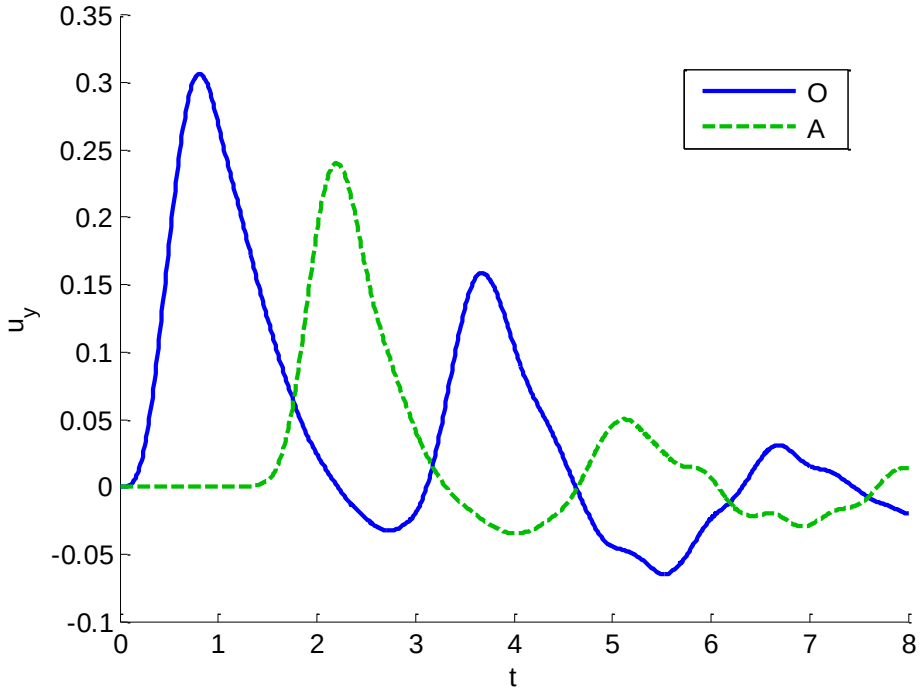

Fig. 10. Vertical displacement at points O and A versus time, impermeable cavity

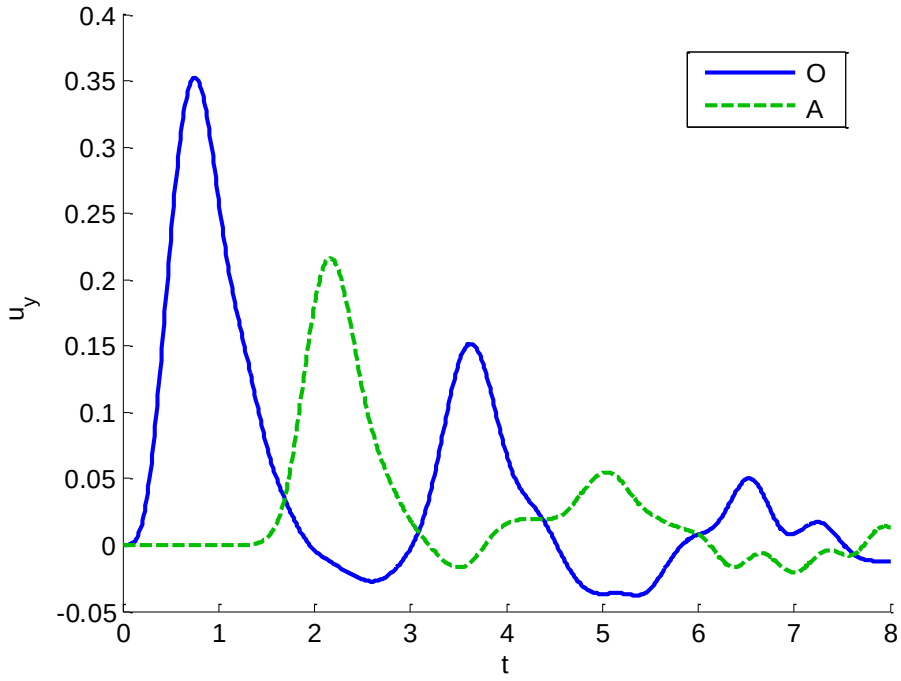

Fig. 11. Vertical displacement at points O and A versus time, permeable cavity

6 Conclusion

Starting with the idea first proposed by Gurtin and Tonti of substituting convolution for inner product operators as the basis for variational formulations for dynamical systems, we present a mixed convolved action approach for Biot poroelasticity. The action functional involves a mixed set of impulsive variables, including skeleton displacement, relative pore fluid displacement, stress impulse and pore pressure impulse, which are selected to provide a well-defined and balanced structure to the formulation. As a result, the mixed convolved action functional, although algebraically complicated, encapsulates all of the governing partial differential equations, boundary conditions and initial conditions of the poroelastic problem. This provides the basis for the *Principle of Stationary Mixed Convolved Action* for a Linear Poroelastic Continuum undergoing infinitesimal deformation. Moreover, a new time and space finite element method

is developed systematically from this framework, which inherits key characteristics of the underlying problem, such as energy conservation for cases without viscous dissipation.

For future work, it will be interesting to investigate further these key characteristics of the finite element representations as the nature of the poroelastic problem shifts from a purely conservative process to one dominated by viscous dissipation. In addition, there is a need to seek a fundamental understanding of the physical meaning of the convolved action and to explore the development of new computational algorithms.

Acknowledgments

The first author (BTD) was supported by the US National Science Foundation (NSF) through the Graduate Research Fellowship Program under Grant Number 1010210. In addition, early portions of this work were funded by NSF under Grant No. CMMI-0900338. The authors gratefully acknowledge this support. However, the results presented here express the opinion of the authors and not necessarily that of the sponsor.

References

[1] Hamilton, W.R., 1834, "On a general method in dynamics," Philosophical Transactions of the Royal Society of London, **124**, 247-308.
[2] Hamilton, W.R., 1835, "Second essay on a general method in dynamics," Philosophical Transactions of the Royal Society of London, **125**, 95-144.
[3] Lanczos, C., 1949, The Variational Principles of Mechanics, University of Toronto Press, Toronto, Canada.
[4] Goldstein, H., 1950, Classical Mechanics. Addison-Wesley Press, Cambridge, MA.
[5] Rayleigh, J.W.S., 1877, The Theory of Sound. I & II. Dover Publications, New York, NY (Second edition, reprint in 1945).
[6] Biot, M.A., 1955, "Variational principles in irreversible thermodynamics with application to viscoelasticity," Physical Review, **97**, 1463-1469.
[7] Biot, M.A., 1957, "New methods in heat flow analysis with application to flight structures," Journal of the Aeronautical Sciences, **24**, 857-873.
[8] Marsden, J.E., Ratiu, T.S., 1994, Introduction to Mechanics and Symmetry: A Basic Exposition of Classical Mechanical Systems, Springer-Verlag, New York.
[9] Gurtin, M.E., 1963, "Variational principles in the linear theory of viscoelasticity," Archive for Rational Mechanics and Analysis, **13**, 179-191.
[10] Gurtin, M.E., 1964, "Variational principles for linear initial-value problems," Quarterly of Applied Mathematics, **22**, 252-256.

[11] Gurtin, M.E., 1964, "Variational principles for linear elastodynamics," Archive for Rational Mechanics and Analysis **16**, 34-50.
[12] Tonti, E., 1973, "On the variational formulation for linear initial value problems," Annali di Matematica Pura ed Applicata, **XCV**, 331-360.
[13] Tonti, E., 1982, "A general solution of the inverse problem of the calculus of variations," Hadronic Journal, **5**, 1404-1450.
[14] Tonti, E., 1984, "Variational formulation for every nonlinear problem," International Journal of Solids and Structures, **22**, 1343-1371.
[15] Tonti, E., 1985, "Inverse problem: Its general solution," In: Differential Geometry, Calculus of Variations and Their Applications, Ed: G. M. Rassias, T. M. Rassias, Marcel Dekker, New York, NY.
[16] Oden, J.T., Reddy, J.N., 1983, Variational Methods in Theoretical Mechanics, Springer-Verlag, Berlin.
[17] Dargush, G.F., Kim, J., 2012, "Mixed convolved action," Physical Review E, **85**, 066606.
[18] Dargush, G.F., 2012, "Mixed convolved action for classical and fractional-derivative dissipative dynamical systems," Physical Review E, **86**, 066606.
[19] Dargush, G.F., Darrall, B.T., Kim, J., Apostolakis, G., 2015, "Mixed convolved action principles in linear continuum dynamics," Acta Mechanica, **226**, 4111–4137.
[20] Dargush, G.F., Apostolakis, G., Darrall, B.T., Kim, J., 2016, "Mixed convolved action variational principles in heat diffusion," International Journal of Heat and Mass Transfer, in press.
[21] Biot, M.A., 1941, "General theory of three-dimensional consolidation," Journal of Applied Physics, **12**, 155-164.
[22] Biot, M.A., 1956, "Theory of propagation of elastic waves in a fluid-saturated porous solid. I. Low frequency range," Journal of the Acoustical Society of America, **28**, 168–178.
[23] Biot, M.A., 1962, "Mechanics of deformation and acoustic propagation in porous media," Journal of Applied Physics, **33**, 1482–1498.
[24] Biot, M.A., 1962. "Generalized theory of acoustic propagation in porous dissipative media," Journal of the Acoustical Society of America, **34**, 1254–1264.
[25] Morse, P.M., Feshbach, H., 1953, Methods of Theoretical Physics, McGraw-Hill, New York.
[26] Riewe, F., 1996, "Nonconservative Lagrangian and Hamiltonian mechanics," Physical Review E, **53**, 1890-1899.
[27] Riewe, F., 1997, "Mechanics with fractional derivatives," Physical Review E, **55**, 3581-3592.
[28] Kaufman, A.N., 1984, "Dissipative Hamiltonian systems: A unifying principle," Physics Letters, **100A**, 419-422.
[29] Morrison, P.J., 1984, "Bracket formulation for irreversible classical fields," Physics Letters, **100A**, 423-427.
[30] Grmela, M., 1984, "Bracket formulation of dissipative fluid mechanics equations," Physics Letters. **102A**, 355-358.
[31] Beris, A.N., Edwards, B.J., 1994, Thermodynamics of Flowing Systems with Internal Microstructure. Oxford University Press, New York.
[32] Grmela, M., Ottinger, H.C., 1997, "Dynamics and thermodynamics of complex fluids. I. Development of a general formalism," Physical Review E, **56**, 6620-6632.
[33] Ottinger, H.C., Grmela, M., 1997, "Dynamics and thermodynamics of complex fluids. II. Illustrations of a general formalism," Physical Review E, **56**, 6633-6655.
[34] Grmela, M., 2014, "Contact geometry of mesoscopic thermodynamics and dynamics," Entropy, **16**, 1652-1686.
[35] Grmela, M., 2015, "Geometry of multiscale nonequilibrium thermodynamics," Entropy, **17**, 5938-5964.
[36] Apostolakis, G., Dargush, G.F., 2013, "Mixed variational principles for dynamic response of thermoelastic and poroelastic continua," International Journal of Solids and Structures, **50**, 642-650.
[37] Predeleanu, M., 1984, "Development of boundary element method to dynamic problems for porous media," Applied Mathematical Modelling, **8**, 378-382.

[38] Manolis, G.D., Beskos, D.E., 1989, "Integral formulation and fundamental solutions of dynamic poroelasticity and thermoelasticity," Acta Mechanica, **76**, 89-104.
[39] Sivaselvan, M.V., and Reinhorn, A.M., 2006, "Lagrangian approach to structural collapse simulation," Journal of Engineering Mechanics, ASCE, **132**, 795-805.
[40] Sivaselvan, M.V., Lavan, O., and Dargush, G.F., Kurino, H., Hyodo, Y., Fukuda, R., Sato, K., Apostolakis, G., Reinhorn, A.M., 2009, "Numerical collapse simulation of large-scale structural systems using an optimization-based algorithm," Earthquake Engineering and Structural Dynamics, **38**, 655-677.
[41] Apostolakis, G., and Dargush, G.F., 2012, "Mixed Lagrangian formulation for linear thermoelastic response of structures," Journal of Engineering Mechanics, ASCE, **138**, 508-518.
[42] Oldham, K.B., Spanier, J., 1974, The Fractional Calculus, Academic Press, New York.
[43] Samko, S.G., Kilbas, A.A., Marichev, O.I., 1993, Fractional Integrals and Derivatives, Gordon and Breach Science Publishers, Switzerland.
[44] Darrall, B.T., Dargush, G.F., 2015, "Mixed convolved action principles for dynamics of linear poroelastic continua," International Mechanical Engineering Congress and Exhibition, IMECE2015-52728, Houston.
[45] Kane, C., Marsden, J.E., Ortiz, M., 1999, "Symplectic-energy-momentum preserving variational integrators," Journal of Mathematical Physics, **40**, 3357-3371.
[46] Kane, C., Marsden, J.E., Ortiz, M., West, M., 2000, "Variational integrators and the Newmark algorithm for conservative and dissipative mechanical systems," International Journal for Numerical Methods in Engineering, **49**, 1295-1325.
[47] Marsden, J.E., West, M., 2001, "Discrete mechanics and variational integrators," Acta Numerica, **10**, 357-514.
[48] Bathe, K.J., 1996, Finite Element Procedures, Prentice Hall, Englewood Cliffs, N.J.
[49] Zienkiewicz, O.C., Taylor, R.L., Zhu, J.Z., 2013, The Finite Element Method: Its Basis and Fundamentals, Butterworth-Heinemann, Oxford, UK.
[50] Chen, J., Dargush, G.F., 1995, "Boundary element method for poroelastic and thermoelastic analyses," International Journal of Solids and Structures, **32**, 2257-2278.
[51] Simon, B.R., Zienkiewicz, O.C., Paul, D.K., "An analytical solution for the transient response of saturated porous elastic solids", International Journal for Numerical and Analytical Methods in Geomechanics, **8**, 381-398.